

# PROCEEDINGS OF SPIE

[SPIEDigitallibrary.org/conference-proceedings-of-spie](https://www.spiedigitallibrary.org/conference-proceedings-of-spie)

## Micro-fabrication of Si-based optomechanical inertial sensors for cryogenic temperatures

Andrea Nelson, Felipe Guzman

Andrea Nelson, Felipe Guzman, "Micro-fabrication of Si-based optomechanical inertial sensors for cryogenic temperatures," Proc. SPIE 11817, Applied Optical Metrology IV, 118170G (5 August 2021); doi: 10.1117/12.2594388

**SPIE.**

Event: SPIE Optical Engineering + Applications, 2021, San Diego, California, United States

# Micro-fabrication of Si-based optomechanical inertial sensors for cryogenic temperatures

Andrea Nelson<sup>\*a b</sup>, Felipe Guzmán<sup>b</sup>

<sup>a</sup>Wyant College of Optical Sciences, The University of Arizona, 1630 E University Blvd, Tucson, AZ USA 85721;

<sup>b</sup>Department of Aerospace Engineering, Texas A&M University, 701 H.R. Bright Building 3141, College Station, TX USA 77843

## ABSTRACT

The design of next generation gravitational wave observatories considers operation at cryogenic temperatures to enhance their sensitivity by reducing thermal noise fluctuations. **Inertial sensors** are used on the observatory platforms to measure local seismic noise and counteract its effects by active control or subtraction in post-processing. Measuring the displacement of a test mass in a resonator system allows for creation of a compact **accelerometer** system. Currently, there are no commercial inertial sensors available that are capable of operating at cryogenic temperatures and providing the required sensitivities for gravitational wave observatories. Materials such as fused silica exhibit very low losses at room temperature. However, this changes significantly at lower temperatures. Unlike fused silica, the Q factor of crystalline silicon structures is expected to remain high at low temperatures, making it a likely candidate for use in these types of inertial sensors. We are working to fabricate compact mechanical resonators from Si wafers to test their mechanical response. **Micro-fabrication** consists of optimizing the photolithography and **Bosch** etching processes for through-wafer Si etching on a 280  $\mu\text{m}$ , 500  $\mu\text{m}$ , and 1 mm wafer. Successful etching on 280  $\mu\text{m}$  wafers has been achieved. We report on the design, model, and fabrication progress of these resonators.

**Keywords:** Inertial sensor, accelerometer, micro-fabrication, Bosch

## 1. INTRODUCTION

Highly sensitive acceleration measurements are a vital aspect in sensor technology. Accelerometers are fundamental in fields such as precision measurement,<sup>1</sup> inertial navigation,<sup>2</sup> and gravitational physics.<sup>3</sup> We work with monolithic optomechanical accelerometers made of fused silica to investigate their precision and sensitivity limits. These accelerometers consist of a resonating test mass and an optical Fabry-Perot (FP) cavity. The cavity is formed between two optical fibers, one attached to the test mass and another to the support structure. Accelerations are measured by monitoring voltage fluctuations from the cavity output due to cavity length changes caused by test mass displacement. The limiting read-out factor is the displacement resolution of the measuring tool, which corresponds to the FP interferometer sensitivity.

This work discusses previously studied highly sensitive accelerometers designed from fused silica with high acceleration sensitivities at room temperature.<sup>1</sup> We address the need for comparable devices fabricated from alternate materials for operation at cryogenic temperatures. Next generation gravitational wave detectors are designed to operate at cryogenic temperatures in order to improve detector sensitivity by reducing the thermal noise fluctuations which dominate at low frequencies.<sup>4 5</sup> Optics at these observatories will be operated down to 20 K or lower.<sup>6</sup> To remove external noise from the system, such as ground motion, accelerometers are used and operated at the same temperature as the core optics. Currently, no commercially available inertial sensors operate at cryogenic temperatures with similar sensitivities. We investigate the use of Bosch etching for fabrication of silicon (Si) resonators for use in accelerometer systems. These Si resonators are monolithic for increased mechanical quality factor (Q) and compact for portability. They could be implemented under such circumstances provided comparable sensitivity is achieved. They could likewise be implemented in other systems which operate at these reduced temperatures, such as the force sensor presented in Melcher et al.<sup>7</sup> Using Bosch etching, we aim to micro-fabricate highly sensitive resonators from Si wafers that are 1 mm thick or greater to test their mechanical properties and read out sensitivities. Successful etches through 280  $\mu\text{m}$  Si wafers have been obtained (Figure 3).

## 2. FUSED SILICA OPTOMECHANICAL ACCELEROMETER

Our current accelerometers are monolithic fused silica resonators. They are used to create a high finesse micro-cavity Fabry-Perot interferometer using single mode fibers cleaved to an angle less than or equal to  $0.3^\circ$ . One of the cleaved fibers is coated with a high reflectivity dielectric coating<sup>8</sup> and secured in a v-groove in the test mass. Another cleaved fiber is aligned in a second v-groove across the gap to form the micro-cavity (red circle in Figure 1c). Both are secured with a UV curing adhesive. These optical read-out micro-cavity devices are “self-calibrating” and permit direct traceability to SI units. This is a result of the device geometry which oscillates in a one dimensional linear motion and allows for the voltage read-out given in equation 2.<sup>9</sup> Having a self-calibrating system removes the need for reference accelerometers which decreases uncertainty.<sup>9</sup> Previous studies of this type of device provided resolutions as low as  $100 \text{ ng}/\sqrt{\text{Hz}}$  to  $1 \mu\text{g}/\sqrt{\text{Hz}}$  above 1 Hz with a Q of  $4.6 \times 10^5$ , mQ products greater than 50 kg, and displacement noise floors at  $10^{-13} - 10^{-12} \text{ m}/\sqrt{\text{Hz}}$ .<sup>1</sup> Figure 1 shows the design and fundamental mode of oscillation which was developed by Guzmán et al.<sup>10 11 12 11 13</sup>

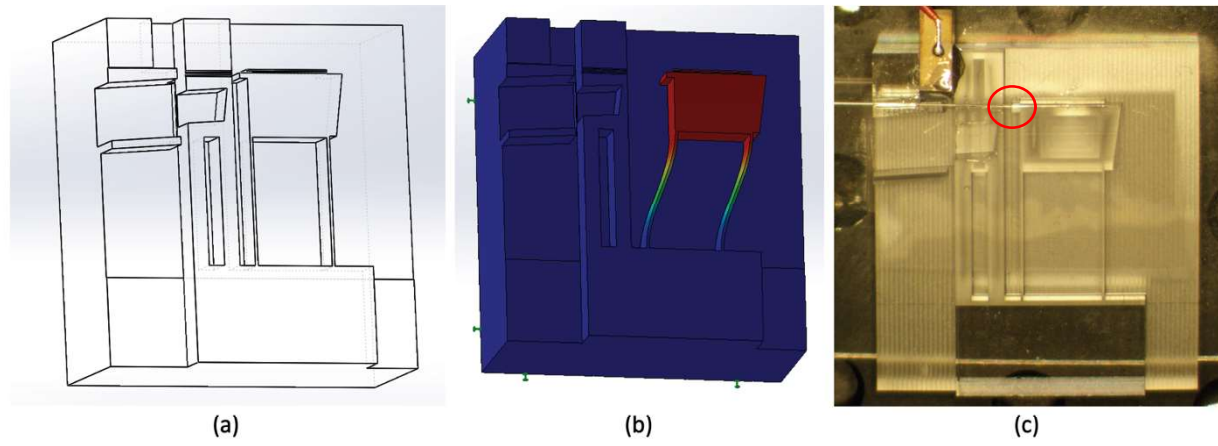


Figure 1: A fused silica resonator model showing (a) the CAD design, (b) the main resonant mode, and (c) an image of the device used to take cavity measurements with the optical fiber cavity circled in red.

### 2.1 Optical Readout

Thermal noise fluctuations in an oscillating test mass define the acceleration resolution limit as given in equation 1.<sup>1 8 14</sup>

$$a_{th} = \sqrt{\frac{4k_B T \omega_0}{m Q}} \quad (1)$$

with  $k_B$  the Boltzman constant,  $T$  the temperature,  $\omega_0$  the natural frequency of the resonator,  $m$  the mass, and  $Q$  the mechanical quality factor. This sets the minimum achievable noise floor.<sup>9</sup> From equation 1, it is clear that a higher  $Q$  and larger test mass reduce this noise floor and result in higher precision. To increase the sensitivity, large values of these two factors are required.

Displacement in the test mass changes the optical cavity length. Cavity fluctuations are related to wavelength fluctuations by  $\frac{dL}{L} = \frac{d\lambda}{\lambda}$  for a scanning FP interferometer.<sup>8</sup> Voltage is dependent on wavelength based on equation 2 with  $\gamma$  the visibility,  $\mathcal{F}$  the finesse,  $L$  the cavity length, and  $\lambda$  the wavelength.<sup>8</sup>

$$V = A \left( 1 - \gamma \frac{1}{1 + \left( \sin^2 \left( \frac{\pi}{2\mathcal{F}} \right) \right)^{-1} \sin^2 \left( \frac{2\pi L}{\lambda} \right)} \right) \quad (2)$$

To determine the acceleration, the oscillation of the test mass is measured using a laser. A circulator directs the light into the cavity, where it is reflected and then read out with a photodetector. Fluctuations in the cavity length  $L$  correspond

with measured voltage fluctuations. This displacement can be converted to acceleration using the transfer function for harmonic oscillators given in equation 3 where  $A(\omega)$  is the acceleration,  $\chi(\omega)$  is the displacement, and  $\omega$  is the angular frequency.<sup>1 8</sup>

$$\frac{\chi(\omega)}{A(\omega)} = -\frac{1}{\omega_0^2 - \omega^2 + i\frac{\omega_0}{Q}\omega} \quad (3)$$

## 2.2 Fused silica cavity characterization

Recent measurements characterizing the optical readout of a duplicate device were done in air. A Newport tunable laser was used to scan the wavelength from 1520 nm to 1570 nm. The voltage response was read out with a National Instruments data acquisition system. Multiple modes were present as seen in Figure 2. Focus was on the modes at 1560.2 nm and 1563.91 nm. Cavity length can be found using the relation  $L = \frac{c}{2 \text{FSR}}$  where FSR is the free spectral range, the separation between adjacent mode peaks. Cavity finesse is the FSR divided by the full width half max (FWHM) of the resonance peak. The FSR was found to be 2.18 THz with a cavity length of 68.8  $\mu\text{m}$ . The mode at 1560.2 nm had a visibility of 57% with a finesse of 63.2. The mode at 1563.91 nm had a visibility of 85.9% and finesse of 77.3. In vacuum ring down measurements will be taken for future comparison with the silicon counterparts. Q factors on the order of  $10^5$  are expected.<sup>1</sup>

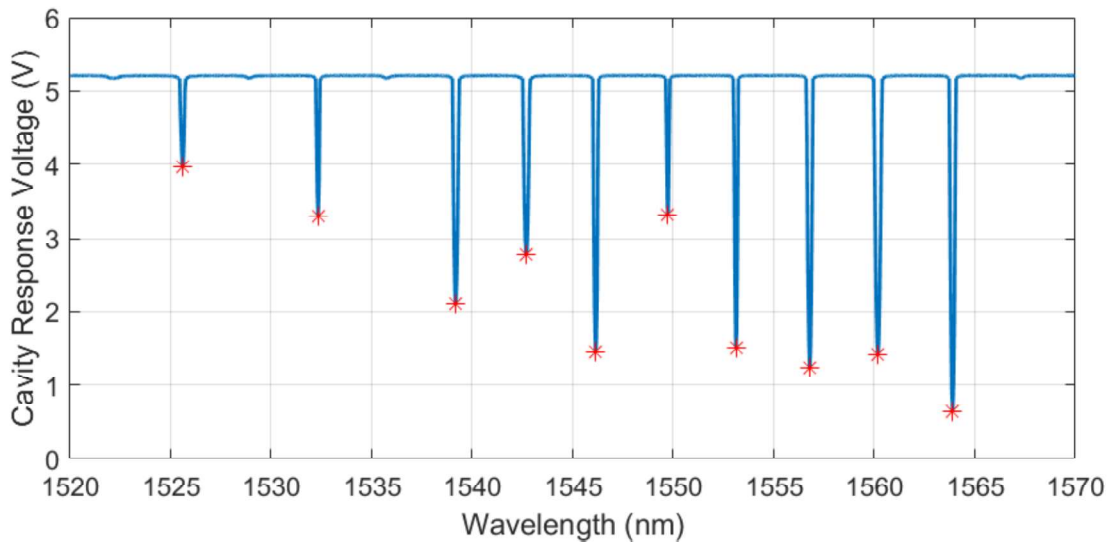


Figure 2: Cavity output voltage due to the scanning of wavelength. Peaks at 1560.2 nm and 1563.91 nm had a visibility of 57% and 85.9% respectively.

## 3. SILICON RESONATOR

Monolithic fused silica resonators are ideal for compact room temperature operation. However, the Q factor of fused silica drops drastically at cryogenic temperatures and is worse at 10 K than 300 K.<sup>15</sup> Since sensitivity is dependent on a high Q, resonators operated at much colder temperatures would need to be fabricated from an alternative material in order to maintain comparable sensitivity. For cryogenic temperatures, the intrinsic Q factor of silicon is at least three orders of magnitude greater than fused silica,<sup>16 17</sup> indicating it is better suited for resonators operating in such environments. Efforts to fabricate comparable resonators from Si wafers are underway.

### 3.1 Fabrication

The Si resonator fabrication process being implemented uses a combination of photolithography and Bosch etching, a form of deep reactive ion etching (DRIE). To date, photolithography was patterned using Heidelberg instruments MLA150 maskless aligner and etching was done using Plasmatherm's Versaline DSE III ICP RIE with  $\text{C}_4\text{F}_8$  and  $\text{SF}_6$  gases for passivation and etching respectively. Fabrication has recently moved location and will soon resume using an EVG 610

double-sided mask aligner and an Oxford Plasmalab 100 ICP RIE system. Two resonators have been successfully etched from a 280  $\mu\text{m}$  wafer with the Plasmatherm Versaline. The flexures broke during the cleaning process, so measurements have yet to be taken with these. Once new devices are able to be fabricated, measurements and characterization similar to that of the fused silica resonators will be conducted.

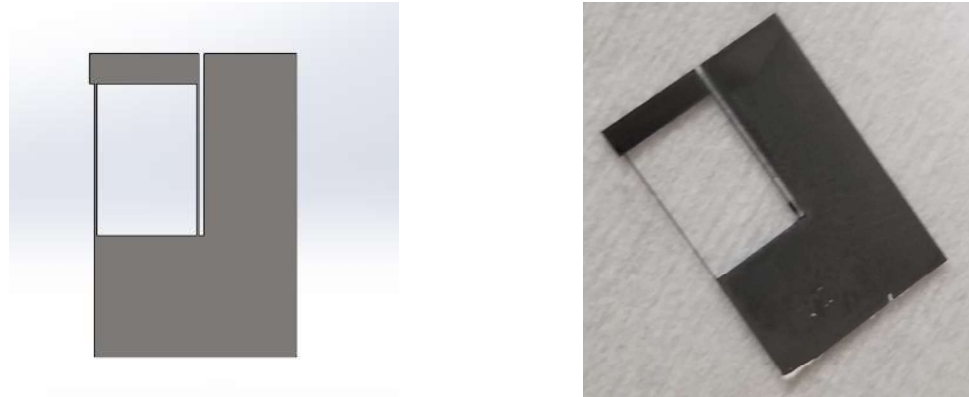


Figure 3: Si resonator design model and resonator etched from a 280  $\mu\text{m}$  Si wafer using the Bosch process.

### 3.2 Modeling

Solidworks and COMSOL software were used to model the resonant frequency of the successfully etched and future Si designs. Modal analysis of the successfully etched geometry (280  $\mu\text{m}$  wafer) shows the fundamental mode  $\omega_0$  at 1.0512 kHz with higher order modes at 1.0843 kHz, 3.8192 kHz, 3.8687 kHz, and 14.912 kHz. Analysis was done using Solidworks finite element analysis (FEA) with a frequency analysis simulation (Figure 4). The test mass of this resonator is roughly 5.39 mg. As previously noted, the thermal acceleration noise floor is inversely related to the mQ product of the resonator by equation 1. A larger test mass indicates a potential for a reduced acceleration noise floor. Therefore, having a larger resonator test mass would allow for better sensitivities. Future fabrication efforts will focus on etching through thicker silicon wafers with similar geometries to obtain larger mQ products to reach higher sensitivities, similar to those obtained with fused silica.

The first higher order mode  $\omega_1$  of the above resonator is not significantly higher than the fundamental mode based on modeling. The fundamental mode  $\omega_0$  is primarily defined by the flexure thickness while the second order mode is influenced primarily by flexure height.<sup>1</sup> Therefore thicker resonator test masses could also allow for higher order modes far from the fundamental mode. This is beneficial for differentiating oscillations during operation and inhibiting the excitation of higher order modes.<sup>1</sup> The second order mode for the 280  $\mu\text{m}$  thick mass is too close to the first order mode to operate ideally. 500  $\mu\text{m}$  and, preferably, 1mm wafers or larger will be used in future fabrication efforts. For the same geometry, modeling shows fabrication from a 500  $\mu\text{m}$  wafer would result in a 1.0526 kHz fundamental mode with higher orders at 1.9207 kHz, 6.3569 kHz, 6.7593 kHz, and 14.938 kHz and a 9.47 mg test mass. With a 1 mm thickness, the main mode is at 1.0574 kHz with higher order modes at 3.7809 kHz, 11.767 kHz, 12.848 kHz, and 15.017 kHz and a test mass of 18.93 mg. Therefore, for a 1 mm thick mass,  $\omega_1 = 3.58\omega_0$ ,  $\omega_2 = 11.13\omega_0$ ,  $\omega_3 = 12.15\omega_0$ , and  $\omega_4 = 14.20\omega_0$ .

In equation 3 test mass displacements are inversely proportional to the square of the mode frequency. Thus, any displacement due to resonance outside the main mode of the system for 1 mm thick resonators will be at least one order of magnitude smaller than the fundamental mode.<sup>1</sup> Clearly, the deeper the achievable etch, the better the resonator geometry and achievable sensitivity. Etch depths of 500  $\mu\text{m}$  using the Bosch process is achievable.<sup>17</sup> In Tang et al. etches up to 1 mm were achieved using a modified Bosch process for through wafer etching,<sup>18 19</sup> This indicates that fabrication of these devices from 500  $\mu\text{m}$  wafers should be possible and etches up to 1 mm are potential.

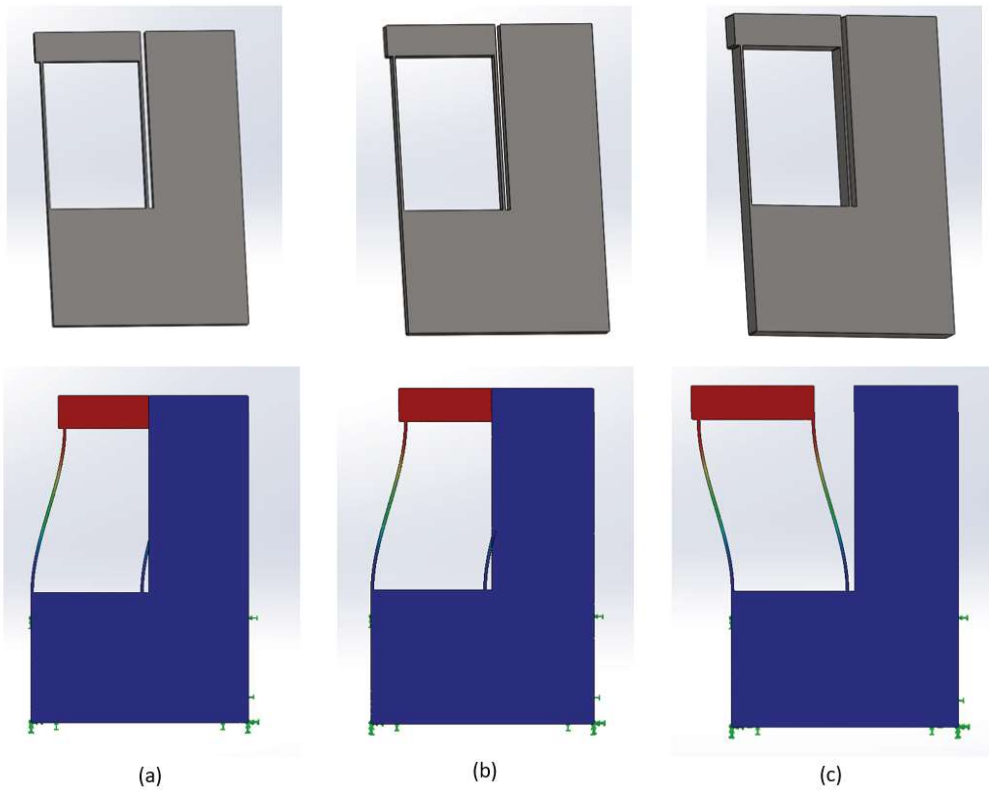


Figure 4: Silicon resonator models and their fundamental mode for resonators fabricated from (a) 280  $\mu\text{m}$ , (b) 500  $\mu\text{m}$ , and (c) 1 mm silicon wafers based on the given geometry.

#### 4. CONCLUSION

This paper discussed existing designs for highly sensitive accelerometers with a FP read-out and introduced the need for comparable resonators that function at cryogenic temperatures. Silicon's higher intrinsic mechanical quality factor at low temperatures make it a promising candidate material. The Bosch method for Si sensor fabrication was discussed, with the successful etching of 280  $\mu\text{m}$  thick resonators presented. Modeling shows the need for thicker resonators, indicating that etches through thicker wafers are necessary, with the ideal 1 mm or larger. A high Q factor paired with a larger mass could allow these compact resonators to perform at high sensitivities at extremely low temperatures, which would allow for their implementation in inertial sensing technologies.

#### ACKNOWLEDGEMENTS:

The authors acknowledge financial support from the National Science Foundation (NSF) PHY-2045579, ECCS-1945832, and OIA-2040575. The Plasmatherm ICP RIE used in etching for this study was acquired by the Wyant College of Optical Sciences cleanroom through an NSF MRI grant – award number ECCS-1725571.

## REFERENCES

- [1] Guzman, F., Kumanchik, L. M., Spannagel, R. and Braxmaier, C., “Compact fully monolithic optomechanical accelerometer,” *5* (2018).
- [2] Dong, Y., Zwahlen, P., Nguyen, A.-M., Rudolf, F. and Stauffer, J.-M., “High performance inertial navigation grade sigma-delta MEMS accelerometer,” *IEEEION Position Locat. Navig. Symp.*, 32–36 (2010).
- [3] Bertolini, A., DeSalvo, R., Fidecaro, F., Francesconi, M., Marka, S., Sannibale, V., Simonetti, D., Takamori, A. and Tariq, H., “Readout system and predicted performance of a low-noise low-frequency horizontal accelerometer,” *Nucl. Instrum. Methods Phys. Res. Sect. Accel. Spectrometers Detect. Assoc. Equip.* **564**(1), 579–586 (2006).
- [4] Shapiro, B., Adhikari, R. X., Aguiar, O., Bonilla, E., Fan, D., Gan, L., Gomez, I., Khandelwal, S., Lantz, B., MacDonald, T. and Madden-Fong, D., “Cryogenically cooled ultra low vibration silicon mirrors for gravitational wave observatories,” *Cryogenics* **81**, 83–92 (2017).
- [5] Hild, S., Chelkowski, S., Freise, A., Franc, J., Morgado, N., Flaminio, R. and DeSalvo, R., “A xylophone configuration for a third-generation gravitational wave detector,” *Class. Quantum Gravity* **27**(1), 015003 (2009).
- [6] Somiya, K., “Detector configuration of KAGRA—the Japanese cryogenic gravitational-wave detector,” *Class. Quantum Gravity* **29**(12), 124007 (2012).
- [7] Melcher, J., Stirling, J., Cervantes, F. G., Pratt, J. R. and Shaw, G. A., “A self-calibrating optomechanical force sensor with femtonewton resolution,” *Appl. Phys. Lett.* **105**(23), 233109 (2014).
- [8] Guzmán Cervantes, F., Kumanchik, L., Pratt, J. and Taylor, J. M., “High sensitivity optomechanical reference accelerometer over 10 kHz,” *Appl. Phys. Lett.* **104**(22), 221111 (2014).
- [9] Gerberding, O., Guzmán Cervantes, F., Melcher, J., Pratt, J. R. and Taylor, J. M., “Optomechanical reference accelerometer,” *Metrologia* **52**(5), 654–665 (2015).
- [10] F. Guzmán et al., “Optomechanical inertial reference for atom interferometers,” International Patent WO 2020/168314 A1 (2020).
- [11] G.A. Shaw, J.M. Taylor, R. Wagner, and F. Guzmán., “Optomechanical reference,” US Patent 10,352,837 (2019).
- [12] F. Guzmán et al., “Beschleunigungsmesssystem (acceleration measurement system),” German Patent No. 102018200052.2 (2018).
- [13] F. Guzmán et al., “Optomechanical gravimeter,” US Patent 10,545,259 B2 (2020).
- [14] Yasumura, K. Y., Stowe, T. D., Chow, E. M., Pfafman, T., Kenny, T. W., Stipe, B. C. and Rugar, D., “Quality factors in micron- and submicron-thick cantilevers,” *J. Microelectromechanical Syst.* **9**(1), 117–125 (2000).
- [15] Schroeter, A., Nawrodt, R., Schnabel, R., Reid, S., Martin, I., Rowan, S., Schwarz, C., Koettig, T., Neubert, R., Thürk, M., Vodel, W., Tünnermann, A., Danzmann, K. and Seidel, P., “On the mechanical quality factors of cryogenic test masses from fused silica and crystalline quartz,” *ArXiv07094359 Gr-Qc* (2007).
- [16] Nawrodt, R., Zimmer, A., Koettig, T., Schwarz, C., Heinert, D., Hudl, M., Neubert, R., Thürk, M., Nietzsche, S., Vodel, W., Seidel, P. and Tünnermann, A., “High mechanical Q-factor measurements on silicon bulk samples,” *J. Phys. Conf. Ser.* **122**, 012008 (2008).
- [17] Hermersdorf, M., Hibert, C., Grogg, D. and Ionescu, A. M., “High aspect ratio sub-micron trenches on silicon-on-insulator and bulk silicon,” *Microelectron. Eng.* **88**(8), 2556–2558 (2011).
- [18] Tang, Y., Sandoughsaz, A. and Najafi, K., “Ultra high aspect-ratio and thick deep silicon etching (UDRIE),” *2017 IEEE 30th Int. Conf. Micro Electro Mech. Syst. MEMS*, 700–703 (2017).
- [19] Tang, Y., Sandoughsaz, A., Owen, K. J. and Najafi, K., “Ultra Deep Reactive Ion Etching of High Aspect-Ratio and Thick Silicon Using a Ramped-Parameter Process,” *J. Microelectromechanical Syst.* **27**(4), 686–697 (2018).